第 30 卷第 5 期 无 机 化 学 学 报 Vol.30 No.5
2014 年 5 月 CHINESE JOURNAL OF INORGANIC CHEMISTRY 969-976

利用吡啶衍生物主配体共轭效应调控铱配合物发光颜色

吴 晨 薛莉莎 李天一 张 松 郑佑轩*
(南京大学化学化工学院,配位化学国家重点实验室,南京微结构国家实验室(筹),南京 210093)

摘要: 利用 2-苯基吡啶及其衍生物为主配体、四苯基膦酰亚胺为辅助配体合成了 3 个铱配合物 $Ir(ppy)_2tpip$(Hppy:2-苯基吡啶,Htpip:四苯基膦酰亚胺)、$Ir(npy)_2tpip$(Hnpy:2-(1-萘基)吡啶)和 $Ir(pnpy)_2tpip$(Hpnpy:2-(9-菲基)吡啶)。它们的结构通过 ^{1}H NMR 和 MALDI-TOF 质谱进行了表征,其中配合物 $Ir(ppy)_2tpip$ 还进一步通过晶体结构分析验证。主配体从苯环到萘环和菲环的改变增加了配合物的 π 共轭,减小了能级差,导致了 3 种配合物的磷光发射光谱从 516 nm 红移到 600 和 633 nm(从绿光到红光),发光量子效率也从 0.36 增加到 0.51 和 0.53。从量化计算的结果可以看出,这种共轭效应增加了主配体的电子密度,提高了配合物的 LUMO 能级。配合物结构和发射性质之间的关系规律为设计不同发光颜色的铱配合物提供了思路。

关键词: 配位化学; 铱配合物; 主配体; 共轭效应; 磷光发射; 红移
中图分类号: O641.4;O641.825 **文献标识码**: A **文章编号**: 1001-4861(2014)05-0969-08
DOI:10.11862/CJIC.2014.146

Color Tuning of Iridium Complexes by Using Conjugative Effect of Pyridine-derived Cyclometalated Ligands

WU Chen XUE Li-Sha Li Tian-Yi ZHANG Song ZHENG You-Xuan*
(*State Key Laboratory of Coordination Chemistry, Nanjing National Laboratory of Microstructures, School of Chemistry and Chemical Engineering, Nanjing University, Nanjing* 210093, *China*)

Abstract: Using pyridine-derived cyclometalated ligands and tetraphenylimidodiphosphinate (Htpip) ancillary ligand, three iridium complexes of $Ir(ppy)_2tpip$ (Hppy=2-phenylpyridine), $Ir(npy)_2tpip$ (Hnpy=2-(naphthalene-1-yl) pyridine) and $Ir(pnpy)_2tpip$ (Hpnpy=2-(phenathren-9-yl)pyridine) were synthesized. Their structures were determined by ^{1}H NMR, MS(MALDI-TOF), and the complex $Ir(ppy)_2tpip$ was also characterized by crystal structure analysis. Extended π conjugation in cyclometalated ligands leads to narrower bandgap resulting in the red shift emission from 516 nm to 600, 633 nm (from green to red). Consequently, when the cyclometalated ligands change from ppy to npy and pnpy, the quantum efficiencies of the complexes are also improved to 0.36, 0.51 and 0.53, respectively. The conjugative effect of the aromatic rings affects the electron density of heterocycle pyridine and thus increases the energy of LUMO as evidenced by the spectroscopic data and the computational calculation results. The regular patterns between the ligand structure and the emission can be applied for designing novel iridium complexes with various colors. CCDC: 966232.

Key words: coordination chemistry; iridium complex; cyclometalated ligand; conjugative effect; phosphorescence; bathochromic-shift

收稿日期:2013-12-12。收修改稿日期:2014-01-06。
南京大学创新训练(No.G1210284036)和国家自然科学基金(No.20971067)资助项目。
*通讯联系人。E-mail:yxzheng@nju.edu.cn;会员登记号:S060015776M。

0 Introduction

The iridium complexes with heterocyclic ligands have been found a wide range of applications in the context of photoactive molecular materials. The strong spin-orbit coupling (SOC) introduced by the central heavy atom can promote the triplet radiative transition, so that such complexes may exhibit unusually high phosphorescence quantum yields at room temperature, as well as relatively short triplet lifetime. Since the phosphorescence of iridium complexes primarily originates from the triplet metal-to-ligand charge transfers (^{3}MLCT) and the ligand-centered (^{3}LC) transitions [1], the energy level of the excited state can be controlled by tuning the energy levels of the ligands through substituent effects, leading to a wide flexible emission color range. Thus, such iridium com-plexes have been widely studied for photocatalysts [2], photochemical solar energy conversion [3], biological labels [4] and, in particular, phosphorescent dopants in the organic light-emitting diodes (OLEDs)[5-8].

According to the density functional theory calculations, the lowest unoccupied molecular orbital (LUMO) is generally localized on the cyclometalated ligands. This suggests that it is useful to modify the cyclometalated ligands to tune the color of the Ir(Ⅲ) complex. Specially, efficient phosphorescent materials based on Ir(Ⅲ) 2-phenylpyridine (Hppy) derivatives have drawn much more attention because they can emit lights in the region of red, green and blue, tuned by modifying ppy cyclometalated ligands as well as by introducing diverse ancillary ligands[1,9-16]. Different substituted groups at different positions of the Hppy ring in Ir(Ⅲ) complexes will result in various spectrum characters.

In this work, we prepared three Ir(Ⅲ) complexes ($Ir(ppy)_2tpip$, Htpip=tetraphenylimidodiphosphinate; $Ir(npy)_2tpip$, Hnpy=2-(naphthalene-1-yl)pyridine; $Ir(pnpy)_2tpip$, Hpnpy=2-(phenathren-9-yl)pyridine) with the modified ppy as the cyclometalated ligands and tpip as the ancillary ligand (Scheme 1). Compared

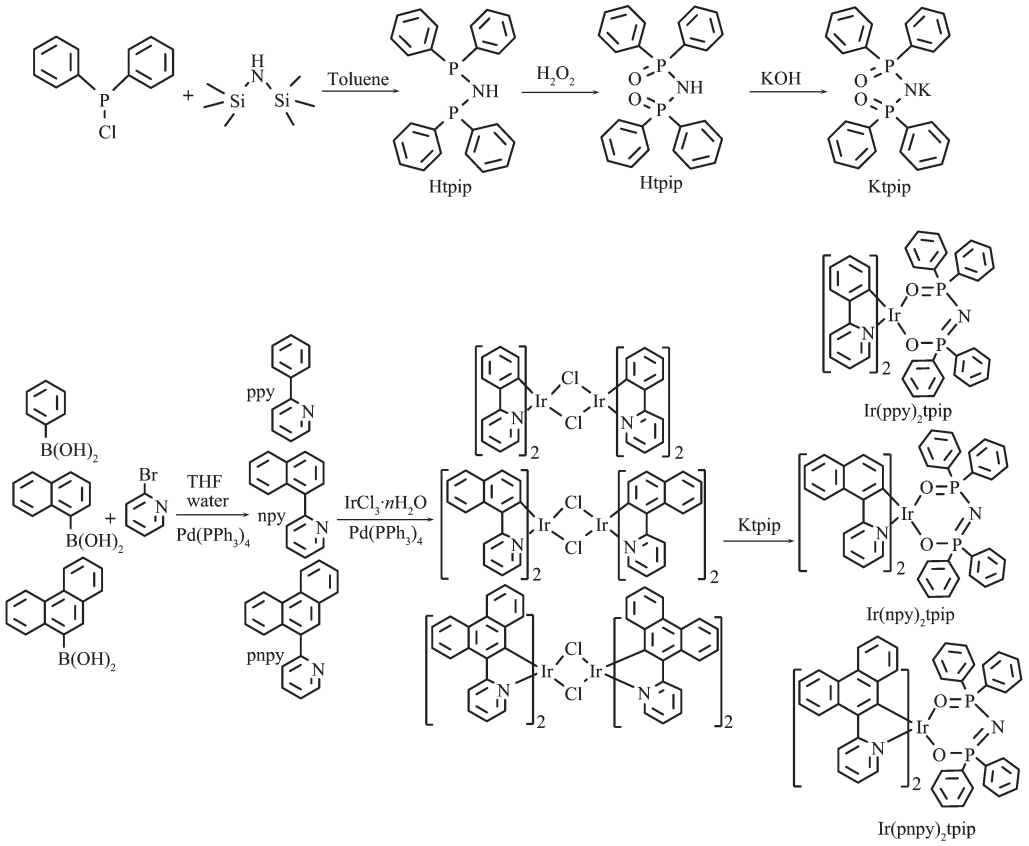

Scheme 1 Synthetic route for the ligands and complexes

with the popular acetonate (Hacac) ligand, tpip derivatives have stronger polar P=O bonds and four bulky aromatic groups, which may improve the electron mobility and lead to larger spatial separation of neighboring molecules of the Ir(Ⅲ) complex to suppress the triplet-triplet annihilation (TTA) and triplet-polaron quenching (TPQ) effectively. The device performances suggest that tpip derivatives are actually useful ancillary ligands for Ir(Ⅲ) complex to benefit their OLEDs performances[17-21]. With the increasing of the conjugated structure of aromatic ring in the cyclomatalated ligands, the emission peaks of these complexes are red-shifted from green to red. Red is one of the three primary colors for full color application. Nevertheless, since the luminescence quantum yields tend to decrease with an increase in the emission peak wavelength, efficient red-emissive complex is not easy to be found[22]. $Ir(npy)_2tpip$ and $Ir(pnpy)_2tpip$ could be the potential materials to fabricate efficient red-emissive OLEDs.

1 Experimental

1.1 General information and materials

The preparation of cyclometalated ligands was based on the Suzuki coupling reaction, which was conducted under the protection of dry nitrogen atmosphere. The thermal properties were evaluated by thermogravimetric/differential thermal analysis (TG-DTA), whose statistics were acquired from the STA 449 F3 (NETZSCH). And the temperature was increased from 30 to 800 ℃. at the rate of 10 ℃·min^{-1}. The high resolution mass spectra measurements (HR EI-MS) were performed on an Agilent 6540 UHD Accurate-Mass Q-TOF LC/MS for all materials. UV-Vis absorption and photoluminescence spectra were both recorded in a dilute $CHCl_2$ solution at room temperature by a Shimadzu 3600 and a Hitachi F-4600 spectrophotometer, respectively. We used Edinburgh FSL-920 spectrophotometer to deliver a laser line (405 nm) with the pulse of 25 ns duration time at 20 Hz repetition rate to obtain the photoluminescence lifetime. Cyclic voltammetry (CV) was used for probing the electrochemical properties of the complexes. The complexes were dissolved in anhydrous CH_3CN with tetrabutylammoniumperchlorate as the supporting electrolyte scanned at a rate of 100 mV·s^{-1}, calibrated by using three electrode cell (a Pt disk working electrode, a Pt wire counter electrode, and a Ag^+/Ag (saturated) reference electrode) assemblies on an IM6ex (Zahner) with ferrocene as the internal standard. The ^1H NMR spectra were recorded on a 500 MHz Bruker AM 500 spectrometer (Bruker Daltonic Inc.) in the solution of $CDCl_3$. Mass spectra (MS) were obtained with ESI-MS (LCQ Fleet, Thermo Fisher Scientific) or MALDI-TOF (Bruker Daltonic Inc.).

1.2 Synthesis and characterization

The syntheses of tetraphenylimidodiphosphinate acid (Htpip) and potassium salt (Ktpip) were according to our previous report[17-21]. CP grade 2-Phenylpyridine (Hppy) was used.

1.2.1 Synthesis of cyclometalated ligands based on pyridine

2-Bromopyridine, boronic acid relatives, $Pd(PPh_3)_4$ and potassium carbonate were heated at 60 ℃ for 6 h in THF and water (1∶1, *V*/*V*) mixture overnight. After cooling, THF was removed by reduced pressure distillation. The product was extracted with CH_2Cl_2 and then dried over anhydrous sodium sulfate. Finally silica column purification (petroleum ether : dichloromethane as eluent, 10∶1, *V*/*V*) gave the desired white product.

2-(Naphthalene-1-yl)pyridine (Hnpy) was prepared from 2-bromopyridine (4 mmol, 0.63 g), naphthylboronic acid (5.4 mmol, 0.93 g), Pd $(PPh_3)_4$ (0.05 mmol, 0.06 g) and potassium carbonate (16 mmol, 2.21 g) as a white solid with a yield of 81.16%. MS (ESI): $[M^+]$ Calcd. for 205.25, Found 206.25. ^1H NMR (500 MHz, $CDCl_3$) δ 8.89~8.77 (m, 1H), 8.13 (d, *J*= 8.0 Hz, 1H), 7.95 (d, *J*=8.1 Hz, 2H), 7.84 (td, *J*=7.7, 1.6 Hz, 1H), 7.66~7.63 (m, 1H), 7.63~7.56 (m, 2H), 7.56~7.47 (m, 2H), 7.39~7.30 (m, 1H).

2-(Phenathren-9-yl)pyridine (Hpnpy) was prepared similarly from 2-bromopyridine (3.33 mmol, 0.53 g), phenanthylboronic acid (5 mmol, 1.11 g), $Pd(PPh_3)_4$ (0.05 mmol, 0.06 g) and potassium carbonate (20 mmol, 2.76 g) as a white solid with a yield of 46.92%.

MS (ESI): [M$^+$] Calcd. for 256.33, Found 256.33. ^{1}H NMR (500 MHz, $CDCl_3$) δ 8.84 (d, J=3.1 Hz, 1H), 8.79 (d, J=8.3 Hz, 1H), 8.74 (d, J=8.2 Hz, 1H), 8.09 (d, J=8.2 Hz, 1H), 7.94 (d, J=7.7 Hz, 1H), 7.90~7.81 (m, 2H), 7.70 (ddd, J=13.9, 7.0, 1.3 Hz, 2H), 7.67~7.60 (m, 2H), 7.58 (t, J=7.1 Hz, 1H), 7.42~7.34 (m, 1H).

1.2.2 Syntheses of Ir(Ⅲ) complexes

According to the classic methods, each of the three ligands (10.47 mmol) and $IrCl_3 \cdot nH_2O$ (4.55 mmol) were dissolved in 2-ethoxyethanol (2-$EtOCH_2CH_2OH$):H_2O (3:1, V/V) and refluxed at 140 ℃ for 20 hr. The precipitates were filtered and washed with ethanol to give the yields of 93.96% $[(ppy)_2Ir(\mu\text{-Cl})]_2$ (yellow solid), 86.36% $[(npy)_2Ir(\mu\text{-Cl})]_2$ (organge-red solid) and 97.68% $[(pnpy)_2Ir(\mu\text{-Cl})]_2$ (orange-red solid), respectively.

Ir(Ⅲ)-chloro-bridged dimers and 3.0 equivalent Ktpip were dissolved in DMF 140 ℃ for 24 hr. Upon cooling, the solvent was removed by reduced pressure distillation. The rest residue was added with CH_2Cl_2 and then was filtered. The filtrate was purified by silica column purification.

$Ir(ppy)_2tpip$ was prepared from $[(ppy)_2Ir(\mu\text{-Cl})]_2$ (0.167 mmol, 0.19 g) and Ktpip (0.5 mmol, 0.23 g) with a yield of 48.1%. MS (MALDI-TOF) Calcd. for $IrC_{46}N_3O_2P_2H_{36}$ [M]$^-$: 916.962, Found: 915.962. ^{1}H NMR (500 MHz, $CDCl_3$) δ 9.07 (d, J=5.2 Hz, 2H), 9.07 (d, J=5.2 Hz, 2H), 7.81~7.72 (m, 4H), 7.68 (d, J=8.0 Hz, 2H), 7.54 (d, J=7.7 Hz, 2H), 7.37 (ddd, J=25.8, 16.6, 8.2 Hz, 11H), 7.16 (t, J=7.3 Hz, 2H), 6.99 (s, 4H), 6.82 (t, J=7.3 Hz, 2H), 6.67 (t, J=7.3 Hz, 2H), 6.61 (t, J=6.5 Hz, 2H), 6.16 (d, J=7.6 Hz, 2H). HR EI-MS Calcd. for [M+H]$^+$: 918.1985, Found: 918.1992; for [M+Na]$^+$: 940.180 4, Found: 940.179 9.

$Ir(npy)_2tpip$ was prepared from $[(npy)_2Ir(\mu\text{-Cl})]_2$ (0.1 mmol, 0.13 g) and Ktpip (0.3 mmol, 0.14 g) with the yield of 22.02%. MS (MALDI-TOF) Calcd. for $IrC_{54}N_3O_2P_2H_{40}$ [M]$^-$, 1 017.078 9, Found: 1015.856. ^{1}H NMR (500 MHz, $CDCl_3$) δ 9.17 (d, J=5.0 Hz, 2H), 8.55 (d, J=8.6 Hz, 2H), 8.36 (d, J=8.3 Hz, 2H), 7.74 (dd, J=11.8, 7.7 Hz, 4H), 7.65 (d, J=7.9 Hz, 3H), 7.56~7.48 (m, 5H), 7.45 (dd, J=11.5, 7.8 Hz, 5H), 7.33 (d, J=7.0 Hz, 3H), 7.21 (d, J=7.3 Hz, 3H), 7.09~6.92 (m, 7H), 6.67 (t, J=6.3 Hz, 2H), 6.20 (d, J=8.4 Hz, 2H). HR EI-MS Calcd. for [M+H]$^+$: 1 018.229 8, Found: 1 018.229 0; for [M+Na]$^+$: 1 040.211 7, Found: 1 040.209 9.

$Ir(pnpy)_2tpip$ was prepared from $[(pnpy)_2Ir(\mu\text{-Cl})]_2$ (0.167 mmol, 0.23 g) and Ktpip (0.5 mmol, 0.23 g) with a yield of 22.72%. MS (MALDI-TOF) Calcd. for $IrC_{62}N_3O_2P_2H_{42}$ [M]$^-$, 1 115.180 4, Found: 700.125 [M-tpip]. ^{1}H NMR (500 MHz, $CDCl_3$) δ 8.56~8.49 (m, 6H), 8.47 (d, J=8.1 Hz, 3H), 8.42 (d, J=5.2 Hz, 3H), 8.35 (d, J=8.4 Hz, 3H), 7.72 (t, J=7.6 Hz, 3H), 7.60~7.48 (m, 6H), 7.47~7.40 (m, 3H), 7.29 (s, 3H), 7.19 (t, J=7.3 Hz, 3H), 6.46 (t, J=7.5 Hz, 3H), 6.39 (t, J=6.3 Hz, 3H), 5.84 (t, J=10.0 Hz, 3H). HR EI-MS Calcd. for [M-tpip]$^+$: 702.164 1, Found: 702.164 2.

2 Results and discussion

2.1 Crystallography of $Ir(ppy)_2tpip$

Suitable single crystal of complex $Ir(ppy)_2tpip$ was mounted on a Brucker SMART APEX CCD diffractometer equipped with a graphite-monochromated Mo $K\alpha$ radiation source (λ=0.071 073 nm) at room temperature using both Φ- and ω-scan modes. Intensity data were collected in the θ range of 1.00~26.00. All absorption corrections were performed with SADABS program. The structure was solved by direct methods and refined on F^2 with full-matrix least-squares and expanded using Fourier techniques. The non-hydrogen atoms were refined anisotropically. Hydrogen atoms were placed in the calculated positions using the riding model. All calculations were performed using the SHELXTL-2000 program package. Single crystal X-ray diffraction analyses show that the complex $Ir(ppy)_2tpip$ crystallizes in the space group $P2_1/c$ of monoclinic system (Fig.1, Table S1). The X-ray crystal structure reveals that the central Ir(Ⅲ) atom occupies an octahedral coordination, which is composed of two carbon atoms and nitrogen atoms from the cyclometalated ligands and oxygen atoms offered by ancillary ligands. The two Ir-C bonds are in a mutually cis-arrangement, whereas the N atoms from cyclometalated ppy are trans-arranged (Table S2).

CCDC: 966232.

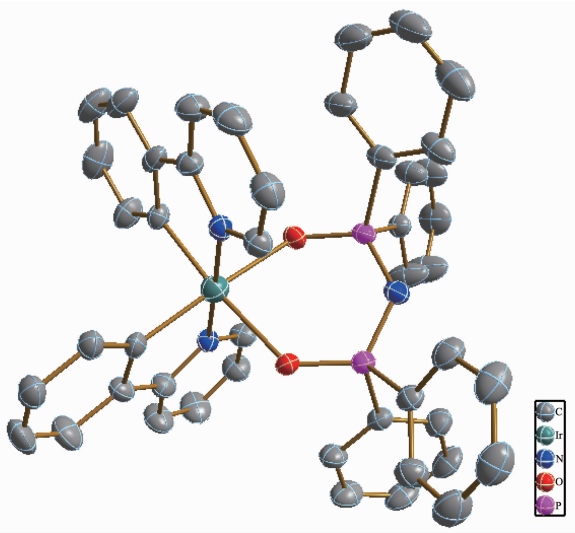

Hydrogen atoms are omitted for clarity. Ellipsoids are drawn at 30% probability level. Crystal data: $C_{46}H_{36}IrN_3O_2P_2$, M_w=916.94, monoclinic, space group $P2_1/c$, a=1.555 16(12) nm, b=1.116 11(9) nm, c=2.349 52(18) nm, $\alpha=\gamma=90°$, β=106.523 0(10)°, V=3.909 7(5) nm^3, Z=4, D_c=1.558 g·cm^{-3}, F(000)=1 824, Flack=0.091(2), GOF=1.000, R_1=0.038 3, wR_2=0.076 6

Fig.1　ORTEP diagrams of Ir(ppy)$_2$tpip with atom -numbering schemes

2.2　UV-Vis spectra and photoluminescence property

In the absorption spectra in CH_2Cl_2 solutions (5 μmol·L^{-1}) at room temperature all complexes show similar features with maxima around λ=225 and 255 nm with shoulders at lower energy (Table 1, Fig.2(a)). Here density functional theory (DFT) calculations were performed using the GAUSSIAN-09 software package (Gaussian, Inc.) at the B3LYP /LANL2DZ level in order to make a comparison between observed and simulated absorption spectra for all complexes. The simulation results indicate that the strong absorption bands in the UV region before 350 nm are attributed to the admix absorptions of spin-allowed π-π^* ligand-centered (LC) transitions. The weaker transitions observed at lower energies (420~530 nm) correspond to singlet metal-to-ligand charge transfer transitions (^{1}MLCT) possibly mixed with triplet metal-to-ligand charge transfer transitions (^{3}MLCT). When the cyclometalated ligands change from ppy to npy and pnpy, the absorption bands of the complexes are red-shifted and the intensities are increased consequently.

As depicted in Fig.2(b), complex Ir(ppy)$_2$tpip in degassed dichloromethane solution (50 μmol·L^{-1}) displays a phosphorescent emission with a peak at

Table 1　Photophysical data and energy levels for the complexes

Complex	Absorption λ_{abs} / nm		Emission λ_{em} / nm[b]	Φ[a]	τ / μs[b]	k / s^{-1}	k_{nr} / s^{-1}	HOMO/LUMO / eV[d]
	Experimental[b]	Simulated[c]						
Ir(ppy)$_2$tpip	225, 262, 340, 406	212, 265, 342	516	0.36	1.94	72 100	442 900	−5.26/−3.00
Ir(npy)$_2$tpip	224, 254, 299, 452	219, 242, 300, 371	600	0.51	2.01	99 600	398 400	−5.20/−2.93
Ir(pnpy)$_2$tpip	256, 307, 379, 457	236, 274, 389	633	0.53	2.52	83 370	313 630	−5.23/−2.87

[a] Assuming a quantum luminescent efficient of Φ=0.4 for fac-Ir (ppy)$_3$, QY error=±5%; [b] All data were measured in the degassed CH_2Cl_2 at room temperature; [c] Simulated absorption data from calculated S_0>T_1 energy based on CH_2Cl_2 as solvent at 298 K;[d] HOMO calculated based on the cyclovoltammetry (CV) diagram by HOMO=−($E_{1/2,ox}$−$E_{1/2,\ Fc+/Fc}$)−4.8 eV, using ferrocene as the internal standard; LUMO calculated based on HOMO and UV-Vis spectra.

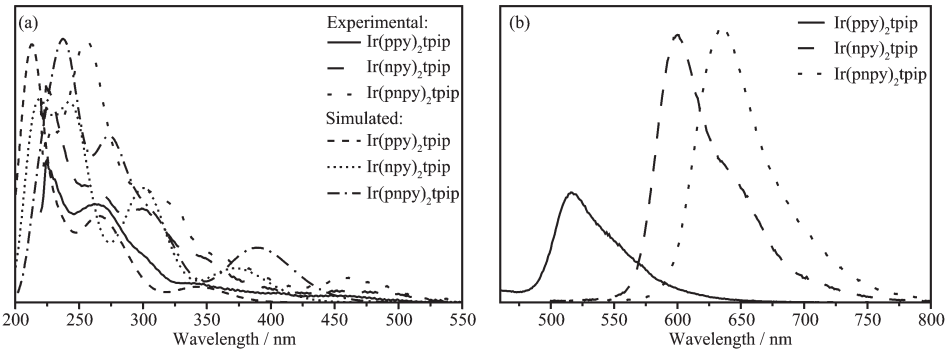

Fig.2　(a) Experimental (solid) and simulated (dash) UV-Vis absorption spectra for complexes in CH_2Cl_2; (b) Emission spectra of the iridium complexes in CH_2Cl_2

516 nm. In comparison, complexes $Ir(npy)_2tpip$ and $Ir(pnpy)_2tpip$ show 84 nm and 117 nm red-shifts, respectively, which indicates that the orientation of π-conjugation would have an influence on the photophysical properties of the phosphorescent complexes. More specifically, the extended π conjugation in cyclometalated ligand leads to a narrower bandgap which makes the emission shift to longer wavel-ength, thus changing the emission color from green to red. Consequently, it is feasible to adjust illuminant color through the modification of the cyclometalated ligands. In addition, when the cyclometalated ligands change from ppy to npy and pnpy, the intensities and quantum efficiencies of the complexes are also improved to 0.36, 0.51 and 0.53, consequently.

The phosphorescence lifetime (τ_p) is the crucial factor that determines the rate of triplet-triplet annihilation in the Ir(Ⅲ) complexes and OLEDs. The longer τ_p of the material usually causes the more severe triplet-triplet annihilation[23]. As indicated in Table 1 and Fig.3, the excited state lifetime of all complexes in the deaerated solutions is monoexponential in the microsecond range which can be assigned to the emission from MLCT states. The luminescence decays of complexes $Ir(ppy)_2tpip$ and $Ir(npy)_2tpip$ are around 2 μs, while complex $Ir(pnpy)_2tpip$ exhibits a longer excited-state lifetime of ~2.5 μs. By using $\Phi_P = \Phi_{ISC}\{k_r/(k_r+k_{nr})\}$ and $\tau_p=(k_r+k_{nr})^{-1}$, it is possible to calculate the radiative (k_r) and nonradiative (k_{nr}) decay rates from Φ_P and τ_P, where the intersystem-crossing yield (Φ_{ISC}) is typically assumed to be 1.0 for metal phosphors with strong heavy-atom effect. The complex $Ir(pnpy)_2tpip$ has the lowest k_{nr} value, which can be expected for the high quantum efficiency.

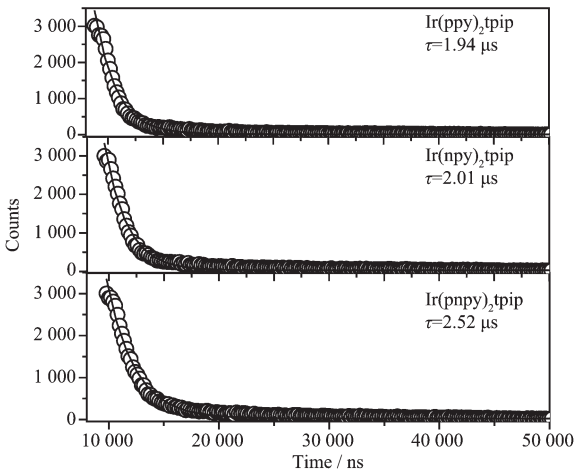

Fig.3 Lifetime curved of $Ir(ppy)_2tpip$, $Ir(npy)_2tpip$ and $Ir(pnpy)_2tpip$

2.3 Electrochemical property and theoretical calculation

The electrochemical behaviors of these Ir(Ⅲ) complexes were investigated by cyclic voltammetry in deaerated acetonitrile at room temperature in order to study the redox property and determine the highest occupied molecular obital/lowest unoccupied molecular obital (HOMO/LUMO) energy levels (E_{HOMO}/E_{LUMO}) using ferrocene as the internal standard (Fig.4). During the anodic scan, reversible one-electron redox peaks at relatively high positive potentials (E_{ox}) of 0.71, 0.68 and 0.70 V for $Ir(ppy)_2tpip$, $Ir(npy)_2tpip$ and $Ir(pnpy)_2tpip$, respectively, can be attributed to metal-centered Ir(Ⅲ)/Ir(Ⅳ) oxidation couple, in accordance with the reported cyclometalated Ir(Ⅲ) systems[24-25]. The ionization potential for the first oxidation (Ir (Ⅲ/Ⅳ)) can be used to establish E_{HOMO} by assuming the absolute level of the Fc (0/I) redox couple (4.8 eV below the vacuum level), and further LUMO energy levels can be calculated from the HOMOs and energy bandgaps obtained from the lowest-energy absorption edges of the UV-Vis spectra, which are 2.26, 2.27 and 2.36 eV for $Ir(ppy)_2tpip$, $Ir(npy)_2tpip$ and $Ir(pnpy)_2tpip$, respectively. Consequently, the HOMO resultant values are −5.26, −5.20 and −5.23 eV for complexes $Ir(ppy)_2tpip$, $Ir(npy)_2tpip$ and $Ir(pnpy)_2tpip$ (Table 1), respectively. The conjugated structure imposes little

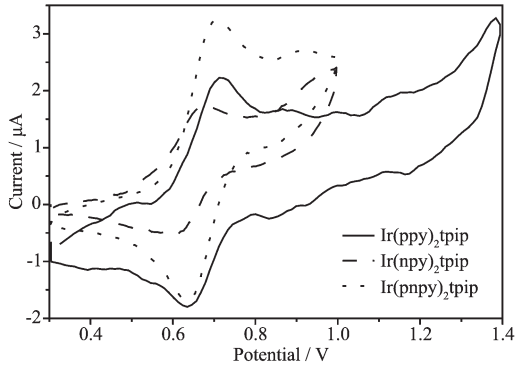

Fig.4 CV spectra of $Ir(ppy)_2tpip$, $Ir(npy)_2tpip$ and $Ir(pnpy)_2tpip$

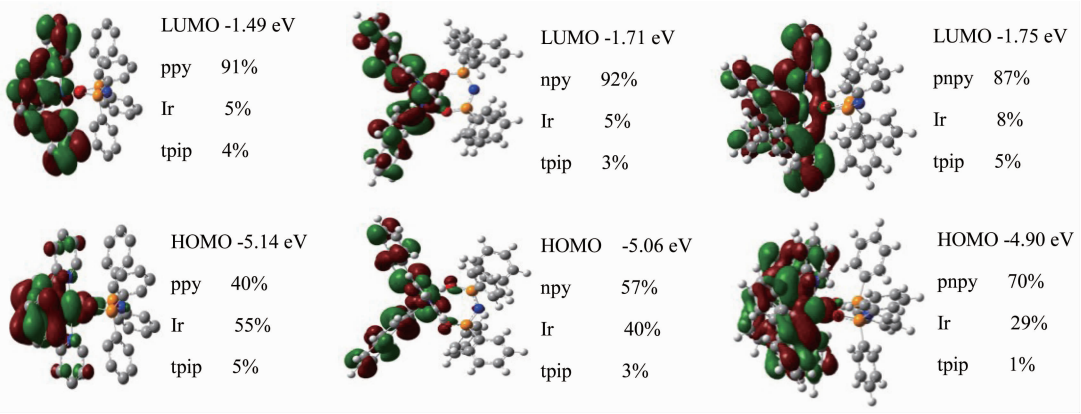

Fig.5 Density functional theory calculation (DFT) results of HOMOs and LUMOs for complexes

impact on the electrons of iridium, hence the HOMOs are almost the same. On the other hand, the electron densities of pyridine are decreased with the extending of conjugation, leading to the shifts of the LUMO data from −3.00 eV to −2.93 and −2.87 eV.

In an effort to elucidate the nature of the electronic transitions within this series of complexes, DFT calculations (computed using the B3LYP hybrid functional) were undertaken. The resultant assessment of the frontier orbitals provides a qualitative insight into the HOMO and LUMO energy levels. Contour plots of the frontier molecular orbitals (FMOs), with the energies and descriptions of them, in terms of % composition of ligand and metal orbitals, are shown and collected in Fig.5. From the point of view of the electronic structure, all the complex models display the typical features of complexes containing iridium atom in a pseudo-octahedral environment.

In particular, the LUMOs are mainly localized on the π-system of ligands and the contributions of pyridyl groups are nearly stable, while the HOMOs are mainly localized on the mixture of pyridyl groups and iridium center. Population analyses reveal that the distributions of the FMOs for all the complexes have similar electron distributions on HOMOs and LUMOs. Specifically, HOMOs consist of the *d* orbitals (29%~55%) of iridium atom and π orbitals (40%~70%) of the cyclometalated ligands, indicating substantial mixing of π orbitals of the ligands with *d* orbitals of metal. What′s more, with the extending of π conjugation, pyridyl groups turn to be a more predominant factor to HOMOs and the ancillary ligand does not contribute remarkably to the LUMOs and HOMOs.

It is worthy to mention that most π orbital contributions from cyclometalated ligands on HOMOs are localized on the phenyl (naphthyl, phenanthyl) and the contribution from the pyridine rings is negligible. But for LUMOs, phenyl (naphthyl, phenanthyl) and pyridine rings share almost the equal contributions. This provides a possible molecular design strategy for such Ir(Ⅲ) complexes with cyclometalated ligands that electron-donating and electron-withdrawing substitutes can be attached to the phenyl (naphthyl, phenanthyl) rings to alter HOMO energy levels, and LUMO energy levels can be altered efficiently when attaching the substitutes to the pyridine rings. Furthermore, the ancillary ligands have little contributions on HOMOs (1%~5%) and LUMOs (3%~5%). As a result, the HOMO-LUMO energy gaps are almost determined by the cyclometalated ligands only, which means that the emission peaks of the complexes are dependent on the phenyl, naphthyl and phenanthyl ligands. The $E_{\text{HOMO-LUMO}}$ values of $Ir(ppy)_2tpip$, $Ir(npy)_2tpip$ and $Ir(pnpy)_2tpip$ are −3.65, −3.35 and −3.15 eV, respect-ively, which are consistent with the bathochromic-shift emission sequence.

3 Conclusions

In this work, we varied the substituents of pyridine to construct different cyclometalated ligands of 2-phenylpyridine, 2-(naphthalene-l-yl)pyridine and

2-(phenathren-9-yl)pyridine. By introducing large conjugative aromatic rings into the ligand, the phosphorescence emissions of $Ir(ppy)_2tpip$, $Ir(npy)_2tpip$ and $Ir(pnpy)_2tpip$ complexes are bathochromic-shifted. Furthermore, the emission intensities and the quantum yields are also increased to 0.36, 0.51 and 0.53. By comparison with the spectroscopic data and the computational results, we can figure that the conjugative effect of the aromatic rings affects the electron density of heterocycle pyridine and thus increases the energy of the LUMO. Those regular patterns of the relationship between the ligand′s structure and the emission can be the guide for designing novel Ir(Ⅲ) complexes with various colors.

References:

[1] Lamansky S, Djurovich P, Murphy D, et al. *J. Am. Chem. Soc.*, **2001**,**123**:4304-4312

[2] Sato S, Morikawa T, Kajino T, et al. *Angew. Chem. Int. Ed.*, **2013**,**52**:988-992

[3] Huang J, Yu J S, Guan Z Q, et al. *Appl. Phys. Lett.*, **2010**, **97**:143301

[4] Tang Y, Yang H R, Sun H B, et al. *Chem. Eur. J.*, **2013**,**19**: 311-1319

[5] Baldo M A, O′Brien D F, You Y, et al. *Nature*, **1998**,**395**: 151-154

[6] Holder E, Langeveld B M W, Schubert U S. *Adv. Mater.*, **2005**,**17**:1109-1121

[7] Gather M C, Kohnen A, Meerholz K. *Adv. Mater.*, **2011**,**23**: 233-248

[8] Kessler F, Watanabe Y, Sasabe H, et al. *J. Mater. Chem. C*, **2013**,**1**:1070-1075

[12]Tamayo A B, Alleyne B D, Djurovich P I, et al. *J. Am. Chem. Soc.*, **2003**,**125**:7377-7387

[13]Tsuzuki T, Shirasawa N, Suzuki T, et al. *Adv. Mater.*, **2003**, **15**:1455-1458

[14]Wong W Y, Ho C L, Gao Z Q, et al. *Angew. Chem. Int. Ed.*, **2006**,**45**:7800-7803

[16]Tao Y T, Wang Q A, Yang C L, et al. *Adv. Funct. Mater.*, **2010**,**20**:2923-2929

[17]Zhu Y C, Zhou L, Li H Y, et al. *Adv. Mater.*, **2011**,**23**:4041 -4046

[18]Teng M Y, Zhang S, Jiang S W, et al. *Appl. Phys. Lett.*, **2012**,**100**:073303-073306

[19]Li H Y, Zhou L, Teng M Y, et al. *J. Mater. Chem. C*, **2013**, **1**:560-565

[20]Xu Q L, Wang C C, Li T Y, et al. *Inorg. Chem.*, **2013**,**52**: 4916-4925

[21]Wang C C, Jing Y M, Li T Y, et al. *Eur. J. Inorg. Chem.*, **2013**:5683-5693

[22]Adachi C, Baldo M A, Forrest S R, et al. *Appl. Phys. Lett.*, **2001**,**78**:1622-1624

[23]Baldo M A, Adachi C, Forrest S R. *Phys. Rev. B*, **2000**,**62**: 10967-10977

[24]Bettington S, Tavasli M, Bryce M R, et al. *Chem. Eur. J.*, **2007**,**13**:1423-1428

[25]Nazeeruddin M K, Wegh R T, Zhou Z, et al. *Inorg. Chem.*, **2006**,**45**:9245-9250